

# Investigation of the failure behavior of a cranial implant-skull model under different load conditions using FEM

<sup>1</sup>Yara Safi, <sup>1</sup>Simone Hohenberger, <sup>1</sup>Christian Robbenmenke, <sup>2</sup>Frans Banki, <sup>2</sup>Bernd Lethaus, <sup>2</sup>Peter Kessler, <sup>1</sup>Thomas Schmitz-Rode, <sup>1</sup>Ulrich Steinseifer

<sup>1</sup> Department of Cardiovascular Engineering, Institute of Applied Medical Engineering (AME), Helmholtz Institute, RWTH Aachen University

<sup>2</sup> Department of Cranio-Maxillofacial Surgery, Maastricht University Medical Center (MUMC), Maastricht

*Abstract: Cranioplasty is a surgical treatment that uses cranial prostheses to restore skull bone defects. However, the reconstruction of large osseous defects is still challenging. A method of treatment was developed at the MUMC in a collaboration of radiologists, computer engineers and cranio-maxillofacial surgeons where Titanium and Polyetheretherketone were used to manufacture the implants. The purpose of the present work - performed at the AME - was to build a simulation model to investigate the effect of stresses on the aforementioned prostheses, with a focus on fixation screws and bone-implant interface. A first simplified model composed of a skull-implant assembly with tangential fixation units was developed, in cooperation with the Maastricht University Medical Center and Engineering Department. The study of two impact scenarios - with high probability of occurrence in a patient's life (e.g., impact of a football, fall on a sharp edge) - was carried out. The mechanical and physical specifications such as contact and interaction properties (e.g. formulation of osseointegration and screw modeling), hyperelastic material definitions, load and boundary conditions were set using the Abaqus CAE tools. The finite element analyses were conducted with Abaqus Standard and Explicit. The results were validated by physical experiments. Hence, a proof of concept was established and more clinically relevant results can be expected with a future implementation of realistic model geometries. This will allow physicians to gain insight into the interaction between prostheses and skull, optimizing the prostheses and thus lowering manufacturing and testing expenses.*

*Keywords: Cranial Implant- Skull Model, Simulation, Experimental Verification, Failure, Fracture behavior, Impact, Implantable medical device*

## 1. Introduction

Large cranial defects result mainly from traumatic head injuries, calvarial tumors or decompressive craniotomies. The consequences for the patient are neurological and psychological problems as well as reduced protection of the brain structure. These ailments are lowered significantly by reconstructing the cranial cavities through a cranioplastic surgery using, if possible, the patient's own bone flap. In case this autologous bone is not re-implantable, a customized alloplastic cranial prosthesis is used (Spetzger 2010). In addition to material biocompatibility, alloplastic implants should have sufficient stability to protect the underlying

brain structure. Moreover, the damage induced by the prosthesis to the surrounding bone tissue in case of external shocks should be kept as low as possible. Various prosthetic materials have been implemented in the past (Winder 2007). Several biocompatibility studies were conducted and the long term outcome was documented (Cabreja 2009).

Since June 2004, 16 patients underwent - at the Maastricht Medical University Center (MUMC) - a cranioplasty where customized implants made out of *Polyetheretherketone* (PEEK) or *Titanium* (*Ti*) were used. These implants were manufactured by Instrument Development Engineering and Evaluation (IDEE, Maastricht). The fixation of the prosthesis to the bone is insured by *tangential* countersunk titanium screws (length 10 mm, diameter 1.5 mm, KLS Martin, Tuttlingen, Germany) Both implant materials seem appropriate to protect the brain against mechanical trauma to a certain extent (Lethaus, 2010). However, to our knowledge, no scientific investigation was conducted to determine the effect of external stresses on the prosthesis regarding brain protection and bone damage.

In order to perform such studies without complicated and expensive experimental investigations, a finite element analysis (FEA) was carried out. The aim of the FEA was to build a *preliminary numerical model* that helps reproducing the medical and surgical setup in order to investigate the structural changes as well as the failure behavior of the skull-implant compound under two different loads conditions: a *pressure* and a *line load*. The *pressure load* could simulate the fall of a paraplegic patient on the ground whereas the *line load* would reproduce an impact with the border of a table or a door. Moreover, the load condition was considered to be a quasi-static one since this assumption can be done at the direct moment of impact. This allowed the use of *Abaqus/Standard*.

## 2. Materials and Methods

Since the human skull is per se, very complex - due mainly to inhomogeneous material and geometry of cranial bones - a simplified model was elaborated for the FEA. However, an effort was made to find the best compromise between the simplifications and the technical specifications.

### 2.1 Geometry and Simulation Units

The setup consisted of a *skull base*, an *implant* and *fixation screws*.

The geometries were constructed using a *CAD/CAM program* and imported to *Abaqus CAE* as an *Elysium Neutral File* (.enf). A ball-shaped design for the whole geometry was set in order to guarantee symmetry and thus lower the computing time.

The roof of the skull base was left out creating a hole, which simulated the craniotomy. Based on average skull geometries (Li 2007) and large sized craniectomies (starting from 100 cm<sup>2</sup>), the inner skull diameter was assumed to be 146 mm and the skull thickness 7 mm. The implant formed the top of the ball and had a thickness of 6 mm (Figure 1 left).

Most cranioplastic surgeries take place six to twelve months after ~~the~~ craniotomy (Winder, 2007), during which bones start remodeling, thus resulting in a round shaped cutting edge. This process was reproduced in the simulation setup through a *bevel bone-implant-interface* (BII) geometry (Figure 1, right), the meshing of a complete round shape being more problematic.

As for the *tangential fixation*, the screw threads were omitted and five bolts with countersunk heads were implemented (Figure 1, right). The diameter of the threadless screw shaft was set to 1.31 mm thus matching the dimensions of the cranioplastic screws (refer § 1).

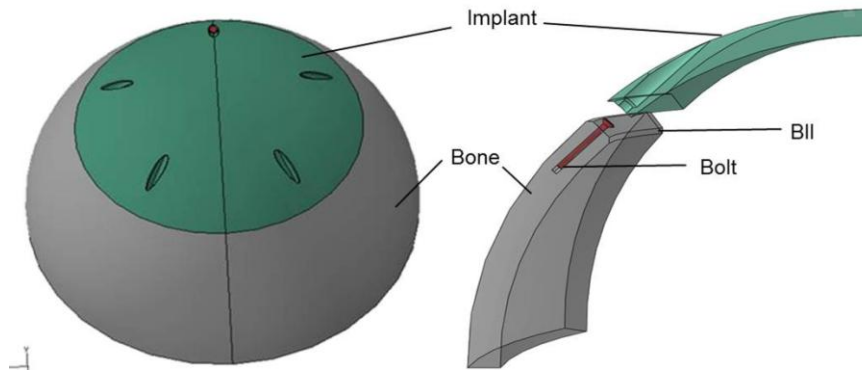


**Figure 1. Skull-implant geometry (left), BII and tangential bolt (right).**

In order to save computational time, only one representative symmetric part of the whole model was considered. Since the model's symmetry conditions change due to the different load applications, two different *simulation units* were implemented (Figure 2). Because the *pressure load* is arranged in a circle on the implant and thus is *rotationally symmetric* like the assembly, *one tenth of the model* was implemented as the pressure load simulation unit – PLSU (Figure 2, left). On the other hand, the only possibility to simulate a *line shaped load* respecting the symmetry conditions was to analyze *one half of the model* for the line load simulation unit - LLSU (Figure 2, right).

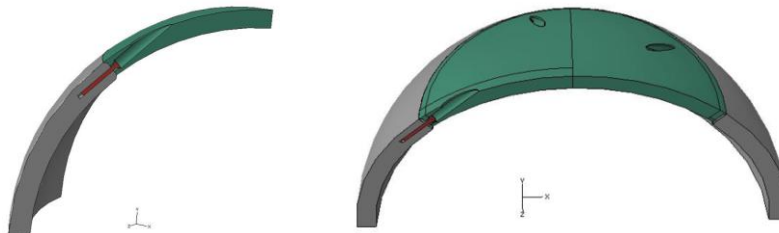


**Figure 2. Pressure (left) and line load simulation units (right).**

## 2.2 Mesh

Since a universal element type is not available, an accurate study of the *element shape* and *order of interpolation* is required.

*Three criteria* were considered for choosing the appropriate element type:

- the ability to mesh the assembly without introducing excessive distortion,
- the expected accuracy of the solution that can be provided with the chosen element, and
- the computational cost.

It is known that *hexahedral elements* usually have a better convergence rate and provide an equivalent accurate result at less cost in comparison to *tetrahedral elements*. *Second-order elements* generally offer a higher accuracy in *Abaqus/Standard*. Nevertheless, the implementation of *first-order hexahedral* elements is recommended for problems involving *contact definitions* (Simulia 2008, 23.1.1; Hughes 2000). Even though extensive attempts in partitioning the geometry were carried out, massive element distortion (for a hexahedral mesh) could not be obviated; *modified tetrahedral elements (C3D10M)* were therefore chosen. Focus was put in generating a homogeneous mesh with growing element density from non-critical areas (the middle part of the bone) to critical ones: around the screw-bone screw interface (BSI) and screw-implant interface (SII) as well as the BII (Figure 3).

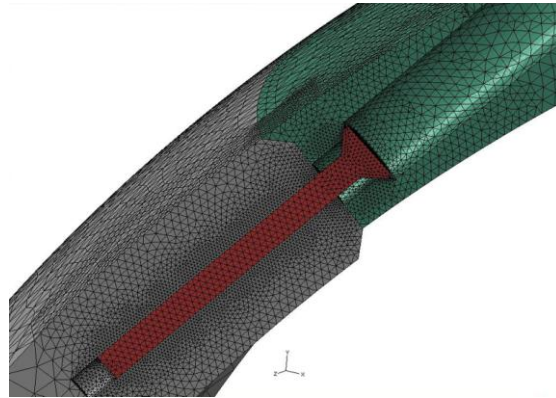


**Figure 3. Mesh density transition between non-critical and critical areas.**

Table 1 shows the element numbers for the PLSU after conducting an extensive *mesh density*<sup>1</sup> in order to find the best compromise between accurate results (hence finer mesh) and computational cost.

**Table 1. Number of elements for the PLSU.**

Part	Area	No. of elements
Bone	BII	2465
	BSI	84436
	Entire part	130729
Implant	BII	35465
	SII	22681
	Entire part	69280
Screw	Entire part	4449

As for the LLSU, the mesh density described previously was not preserved due to the insufficient computation resources since the LLSU is five times bigger than the PLSU.

Thus, a new mesh was generated taking into account the necessity of a high mesh density at the contact surfaces and the load application area. However, a warning free mesh could not be

<sup>1</sup> *Convergence of the Von Mises Stresses within a limit of 10% as practiced in the industry*

achieved. Table 2 gives an overview of the elements generated for the different parts and the warnings in percent.

**Table 2. Number of elements and warnings for the LLSU.**

Part	No. of elements	Warnings [%]
Bone	104374	0
Implant	217911	0.0014
Screw	1359	0

### 2.3 Material definition

The considered skull part - the calvaria - consists of flat bones composed of a thin cancellous bone layer embedded between two layers of cortical bone. As the major part of the skull bone is cortical, the cancellous bone was neglected. For simplification purposes and based on the work of Debolé M. in “Modeling bone tissue fracture and healing: a review”, the *bone material properties* were assumed to be *homogeneous, isotropic* and *linear elastic*. Furthermore, equal strength in tension and compression within the material model are anticipated. Using the *material definition options for a linear elastic behavior* in *Abaqus/CAE*, a Young’s modulus of  $E = 4000$  MPa, an ultimate strength of  $\sigma_{\max} = 205$  MPa and a Poisson’s ration of  $\nu = 0.3$  were assigned. These values are based on experimental values used in recent skull finite element (FE) studies (Motherway 2009).

The choice of the material used - Ti “Alpha-Beta-Alloy Grade 5” and PEEK-OPTIMA - was made in accordance with the medical situation of the patient, the medical history, and the patient’s wishes. PEEK resembles bone more than Titanium (Eschbach 2000) and is more elastic, whereas titanium has a higher yield and ultimate strength, which makes it more inert (Cabreja 2009). Here also, *linear elastic material properties* were set using the *edit material definition dialogue*. The values for PEEK and Ti were taken out of the material datasheets. A summary of the values entered in *Abaqus/CAE* is presented in Table 3.

**Table 3. Material definition for bone, Ti and PEEK.**

Material	Bone	Ti -6Al-4V	PEEK-Optima
Mechanical Properties			
Young’s Modulus [MPa]	4000	110300	4000
Tensile Strength [MPa]	205	675	100
Poisson’s Ratio	0.3	0.36	0.4

### 2.4 Boundary and load conditions

#### Symmetry boundary conditions

The PLSU consisted of one tenth of the whole assembly. Predefined “types” of boundary conditions (BC) were used for the implementation of the symmetric constraints describing this partition. At the right symmetry edge (see Figure 4 right) an *XY-plane symmetry* was reproduced by the *plane symmetry type ZSYMM*. As for the left side, a rotationally symmetric BC around the Y-axis was applied (*YASYMM*).

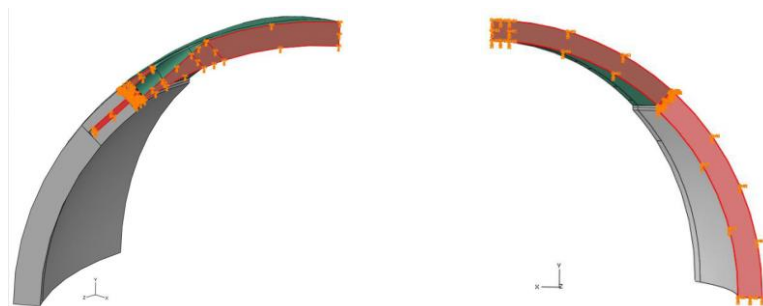


**Figure 4. Surface definition for BC at right (left) and left symmetry plane (right).**

In order to avoid interferences with the screw's interaction definitions and thus over-constraint warnings, the slave nodes of the screw constraints needed to be skipped. To do so, the BC definition at the left side of the assembly was split into two parts: a geometry based assignment at the implant and screw area (see Figure 4 left) and a node based definition at the left skull side (see Figure 5).

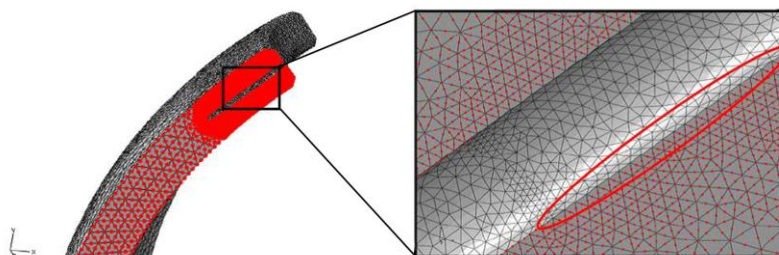


**Figure 5. Node set at left skull side.**

For the LLSU the rotational symmetry of the model could not be used due to the line shaped load condition. Thus only the plane symmetry could be applied: The assembly is cut in the middle which results in an XY-plane symmetry, defined by the *ZSYMM* BC (suppress displacement in Z-direction as well as the rotation around the X and Y-axis). Figure 6 shows the geometry based BC which was applied to the right skull symmetry surface as well as to the implant and the screw. The left skull side was defined via a node set (to avoid over-constraints, refer Figure 5).

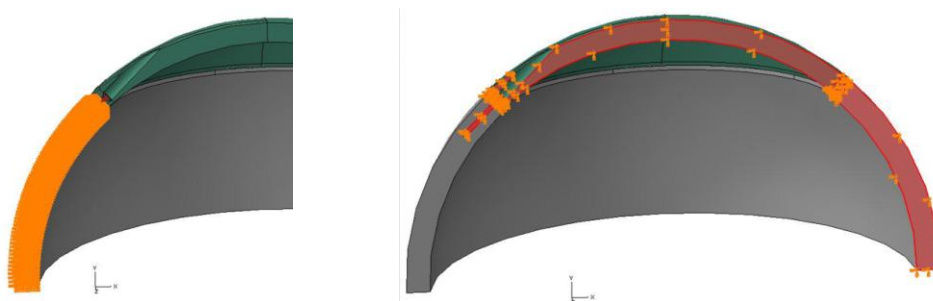


**Figure 6. BC sets for the LLSU: node set (left) and geometry based (right).**

### Fixation boundary conditions

At the lower skull model side, the transition from calvarial bone to the endocranium had to be reproduced. Since the endocranium is very rigid due to several stiff bones, total anchorage is assumed at this position. Thus, a *total built-in constraint (ENCASTRE)* was applied so that neither displacement in X-, Y- or Z-direction nor rotation around the X-, Y- or Z-axis is possible. This definition was used for the PLSU as well as the LLSU.

### Interaction properties

In order to define the *contact between two part instances* in Abaqus/CAE an *interaction module* - where mechanical or thermal interactions between two surfaces are specified - had to be set. In the following setup, three contact pairs are present: BSI, BII and SII. In order to characterize the contact pairs, an *interaction property* is assigned to each *interaction pair*.

#### Bone-screw interface- BSI

As described earlier, the screw threads were neglected and a bolt was modeled. Nevertheless, mechanical properties of the threads had to be implemented. To do so, the surfaces between bone and screw shaft were considered to stick together throughout the whole analysis without any relative motion. In *Abaqus/Standard* two methods are available to realize this condition: a *“Rough” contact (RC)* and a *tie constraint*. Through a RC definition, the friction coefficient is set to infinite so that slipping between the two surfaces does not occur regardless of the contact pressure (Simulia 2007, 15.14.1). Bonding between the surfaces is accomplished with a tie constraint. By equalizing the translational and rotational motion for the contact pair, this method guarantees relative motion suppression between the surfaces within the simulation time (Simulia 2007, 29.3.1). In order to determine the best method, both interaction types were implemented and analyzed. Although the Von Mises Stresses distribution can be considered almost equal in both cases the accuracy of the bondage between the surfaces was not satisfying for the RC: as shown in Figure 7, the screw shaft surface lifted off from the skull surface on the upper screw part; moreover, a penetration of the screw into the skull surface could be detected at the lower screw part.

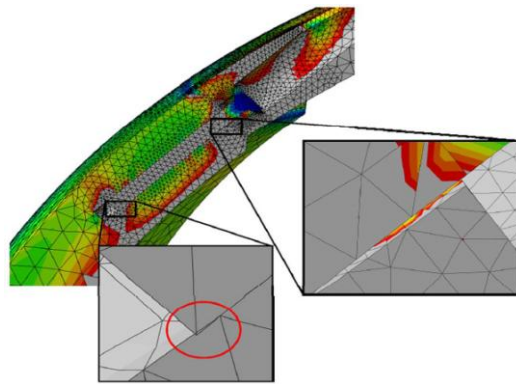


**Figure 7. Stress distribution and surface bondage for RC.**

In comparison to the RC, the tie constraint secured an unflinching bondage throughout the simulation. Thus, the tie constraint was implemented for the BSI.

## Bone-implant interface - BII

Titanium and PEEK imply different interaction behaviors at the BII since a partial bone ingrowth into Ti is given (Albrektsson 1981) whereas PEEK is assumed to be non-osteoconductive (Katzner 2002). Thus, the interaction properties between implant and bone had to be modulated specifically.

### PEEK Implant

The non-osteoconductivity of PEEK implies that *the only interaction* between a PEEK implant and the calvarial bone is a *frictional* one. In order to set this condition, the *Coulomb friction model* was chosen. In its basic form a critical shear stress  $\tau_{crit}$  is defined as:

$$\tau_{crit} = \mu * p \quad \text{Equation 1}$$

where  $\mu$  = friction coefficient and  $p$  = contact pressure.

Up to  $\tau_{crit}$ , no relative motion occurs between the contacting surfaces (sticking) whereas relative surfaces sliding starts for shear stresses  $\tau > \tau_{crit}$ . In *Abaqus/Standard* the *friction model* can be implemented by using a *stiffness (Penalty) method* or a *Lagrange multiplier*. Abaqus recommends the Lagrange multiplier only for problems where the stick/slip behavior resolution is very important (Simulia 2008, 31.1.5) since the computational costs is higher. Hence, the *Penalty method* was implemented. The *friction coefficient* was set to  $\mu = 0.2$  and considered as *directionally isotropic*. Furthermore, the *maximal elastic slip* was chosen as the default value of 0.5% of the characteristic surface dimension. A shear stress limit was not defined.

### Ti implant

In this case, a partial osseointegration of the bone into the implant is expected. Although no studies about the ingrowth rate of calvarial bone into Ti-protheses are available, a proportion of 40% was assumed based on studies of dental Ti implants (Barros 2009). This partial ingrowth was achieved in Abaqus by partitioning the contact surfaces in two areas (Figure 8). The outer area (red) represents 40% of the contact surface and stands for the region of total ingrowth. The inner contact surface assumes the role of non-osteoconductive behavior involved in the interaction pair. *For the osseointegration of bone* into the implant, a *severe bonding* between the contact surfaces throughout the analysis was assumed so that *no relative motion* between the surfaces occurs. Like in the case of the BSI, a *tie constraint* was implemented for this purpose.

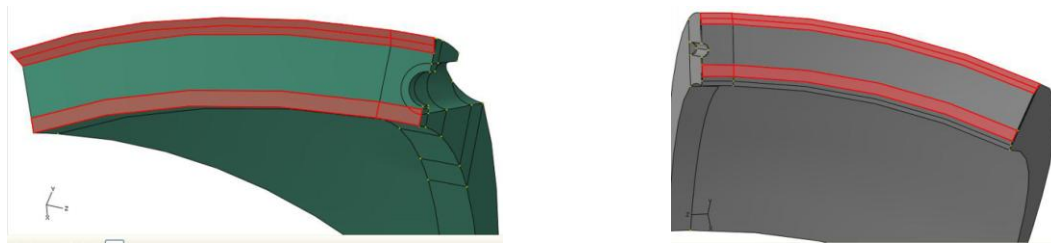


**Figure 8: Surface partition for osteoconduction ingrowth simulation: implant (left) and bone (right)**

Moreover, for the non-osteoconductive area the same conditions as for the PEEK implant were set: *The Penalty method based on the Coulomb friction definition.*



### Screw-implant interface - SII

Since the calculation of the stress distribution in the screw threads causes an increase of the computation time without providing significant extra benefit, the screw shaft was designed as a bolt. By using proper boundary conditions (BCs) a realistic screw model could be implemented. A bolting torque for the screws was not considered, since it mainly depends on the surgeon's practice. Also, the only interaction behavior that was accounted for the SII is a frictional one. Same as for the PEEK implant, the *Penalty method* was applied to this interface. For both implant materials the coefficient of friction was set to  $\mu = 0.2$  and a maximal elastic slip of 0.5 % of the characteristic surface dimension were chosen.

In order to complete the contact definitions for the BSI, BII and SII, a contact formulation was assigned to each interaction pair. Therefore, a 'master' and a 'slave' surface were defined based on the following criteria (Simulia 2008, 30.2.1):

- The slave surface should be assigned to the smaller area
- The master surface should be assigned to the stiffer body
- The master mesh should be coarser than the slave mesh

Table 4 gives an overview of the contact formulation assignment.

**Table 4. Contact formulation assignment.**

Interaction property	Master surface	Slave surface
BSI	Screw shaft	Bone
BII	Implant	Bone
SII	Screw head	Implant

### Load conditions

For the activation of the load conditions, a "load" step had to be defined at first. Due to the fact that large displacements as well as boundary nonlinearities are expected in the analysis, the *nonlinear geometry option (NLgeom)* was activated. Table 5 shows the implemented values for the load step options.

**Table 5. Implemented values for "load" step.**

Parameter	"Load" step
Maximum increment number	1000
Initial increment size	0.0001
Minimum increment size	$1 \cdot 10^{-7}$
Maximum increment size	1

### Pressure load

The pressure load application simulates the hit onto a surface. Therefore, a surface with the radius  $r = 30$  mm was used as the application area (see Figure 9).

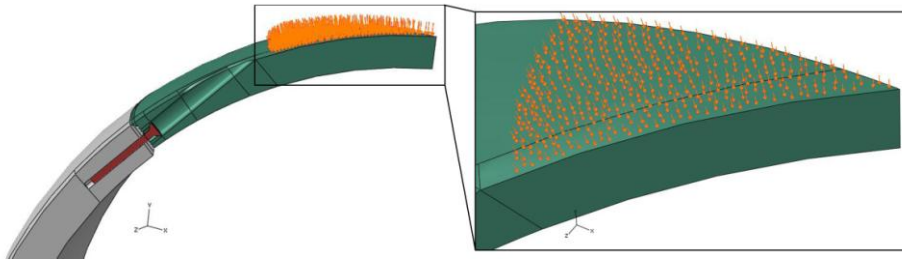


**Figure 9. Application area for pressure load.**

Since neither previous stress/displacement FEAs for cranial implants nor real model tests were available, the load magnitude until total breakthrough of one assembly part was unknown and had to be adapted subsequently. Based on the experience gained from a first model, the starting point was set to a magnitude of  $p = 5$  MPa for the PEEK implant and  $p = 15$  MPa for the Ti implant. The loads were successively increased until an assembly failure could be determined.

Line load

In order to simulate the collision with a sharp edge, a line-shaped load was applied to the assembly. Since the option *to implement a line load is only available for shell elements in Abaqus/Standard*, another load definition had to be set. By defining *concentrated forces* on each line node, the reproduction of a line shaped load was achieved. The length of the line load was set to the value of  $l = 28$  mm. Thus, the comparison between the two load conditions was possible. The application area for the concentrated forces was defined by a node set. By defining the load magnitude for each force in negative Y-direction, the total force could be calculated by the following formula:

$$F_{\text{total}} = n * F_{\text{node}} \quad \text{Equation 2}$$

where  $n$  is the total node number. The node set contained 100 nodes on the half implant unit. A starting point for the investigation was set through the comparison with the pressure load.

The two load conditions mentioned before (a pressure - dull impact and a line load - sharp strike) were applied with a  $90^\circ$  angle, since the tangential component of a bevel force is absorbed by the scalp.

## 2.5 Experimental validation

In order to validate the results of the FEA, an experimental test rig was prepared using a material testing machine and four physical samples (two of each implant material). To reproduce as accurately as possible the set-up of the FEA model, care was taken in the manufacturing of the testing samples as well as the choice of the testing machine. The geometry of the physical samples was identical to the one used in the FEA. Four skull models were manufactured at Materialise (Leuven, Belgium) out of sintered polyamide (PA). PA was chosen because of the similar values of the mechanical properties to the one assumed for the bone model. The implants made of Titanium (Ti-6Al-4V) and of PEEK optima© (Invisio, Lancashire, UK) were manufactured at IDEE. The outer and inner edges were flattened in the polyamide model exactly like the BII and SBI. An extension of the implants was fitted in the external immersion of the model. Moreover, all implants were fixated with five countersunk titanium screw.

The models and test specimens were placed in a standard testing machine and fixated by a custom-made aluminum plate to inhibit movement (Figure 10). The models were subjected to a load (with a quasi-static loading rate of 1.925 mm/min) by moving the lower shaft upwards until structural failure of the sample. The pressure course and the corresponding displacement were measured. All tests were recorded by a high-speed camera with a frame rate of 1000 frames per second. After structural failure, the debris was collected and further investigated.

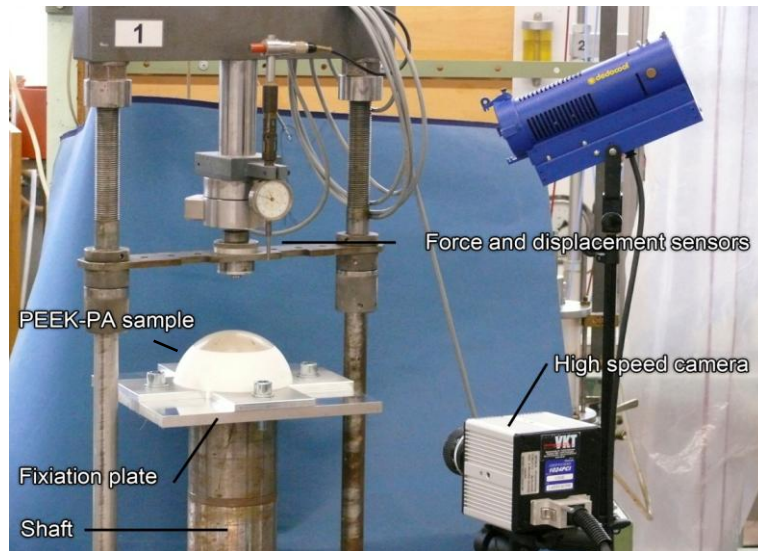


**Figure 10. Experimental test rig with fixated PEEK-PA sample.**

### **3. Results**

In order to assess the structural changes as well as the failure behavior of the skull-implant compound, the Von Mises Stresses were contemplated for each implant as well as for each load situation. Two specific points were considered important for the evaluation: the load force which causes the first plastic change in the material (i.e. the induced stresses are higher than the tensile strength of the material) and the one causing a total break through. Since the location of the possible failure area could not be foreseen, a stress analysis of the whole setup is carried out. As all assembly parts have a different tensile strength (refer Table 3), the result analysis is accomplished individually for bone, implant and screws. An example of the evaluation in the *Output Data Base* (ODB) is given only for the PEEK implant for the pressure load scenario in Figure 11.

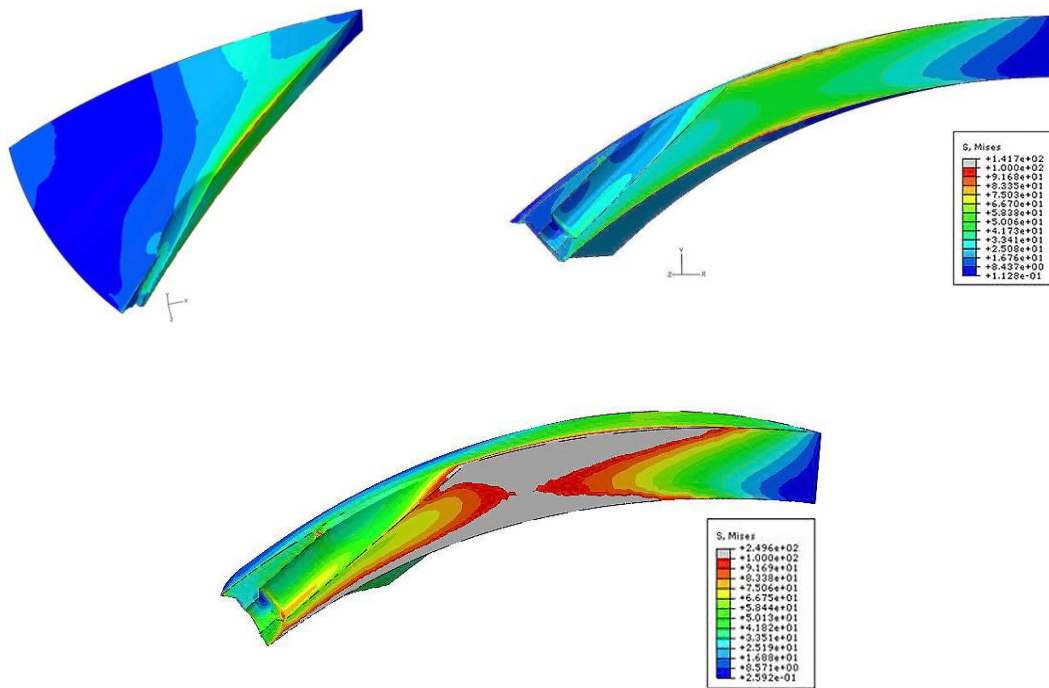


**Figure 11. Von Mises Stress of PEEK implant respectively for  $p = 5$  MPa (up), and  $8.5$  MPa (down).**

Due to the page limitation of this article, the results are listed only in a table form (see Table 7 to Table 10) and the single figures for every case are omitted.

**Table 7. Results for pressure load on PEEK-implant.**

Magnitude [MPa]	Bone ( $\sigma_{\max} = 205$ MPa)	Implant ( $\sigma_{\max} = 100$ MPa)	Screw ( $\sigma_{\max} = 675$ MPa)	Displacement [mm]
5	-	First el. exceeding	-	0.9
6	-	Some el. exceeding	-	1
8	-	Several el. exceeding	-	1.4
8.5	-	Breakthrough	-	1.5

**Table 8. Results for pressure load on Ti-implant.**

Magnitude [MPa]	Bone ( $\sigma_{\max} = 205$ MPa)	Implant ( $\sigma_{\max} = 100$ MPa)	Screw ( $\sigma_{\max} = 675$ MPa)	Displacement [mm]
15	First el. exceeding	First el. exceeding	First el. exceeding	0.5
17.5	Some el. exceeding	Some el. exceeding	Some el. exceeding	0.6
18.5	Some el. exceeding	Some el. exceeding	Several el. exceeding	0.6
20	Some el. exceeding	Several el. exceeding	Breakthrough	0.7

**Table 9. Results for line load on PEEK-implant.**

Magnitude [N/node]	Bone ( $\sigma_{\max} = 205$ MPa)	Implant ( $\sigma_{\max} = 100$ MPa)	Screw ( $\sigma_{\max} = 675$ MPa)	Displacement [mm]
35	-	-	-	1
50	-	First el. exceeding	-	1.5
70	-	Several el. exceeding → Breakthrough	-	2.3

**Table 10. Results for line load on Ti-implant.**

Magnitude [N/node]	Bone ( $\sigma_{\max} = 205$ MPa)	Implant ( $\sigma_{\max} = 100$ MPa)	Screw ( $\sigma_{\max} = 675$ MPa)	Displacement [mm]
300	-	-	-	1.1
350	Some el. exceeding	Some el. exceeding	-	1.3
375	Some el. exceeding	Several el. exceeding → Breakthrough	-	1.4

Moreover, the force and displacement were registered during the experimental validation. The graphs in Figure 12 shows a comparison of the course of deflection and force registered with increasing load between the experimental validation and FEA<sup>2</sup>.

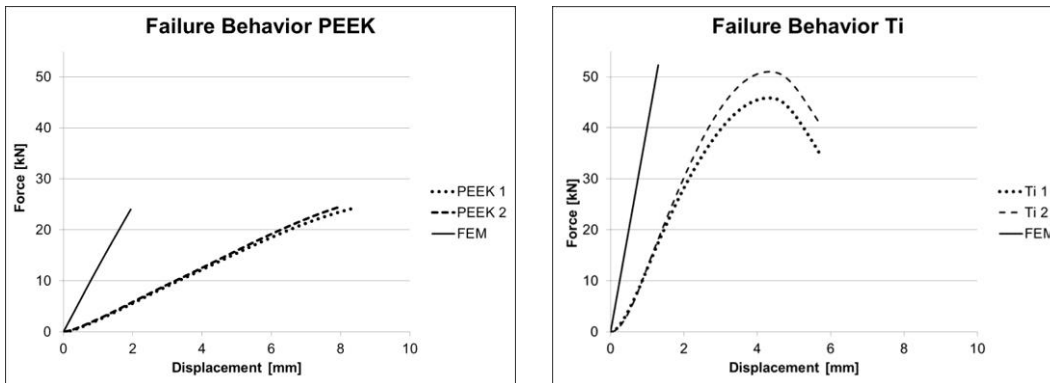


**Figure 12. Force/Deflection curve of PEEK and Ti samples**

## 4. Discussion

In order to be able to compare the results for the pressure and line load, the loads were converted into the total force that impacts on the assembly.

Since the pressure load is applied normal to the round shaped implant surface, the total force is calculated by the formula:

$$F = p \cdot A \quad \text{Equation 3}$$

where A is defined as the projected area of the load application surface with the radius  $r = 30$  mm (see § 2.1). The total line load force can be calculated by the Equation 2.

Table 11 gives an overview of the maximal impact forces as well as the failing part for the different materials and loads. Table 12 resumes the maximal implant displacement.

<sup>2</sup> After implementation of the PA material properties

**Table 11. FEA results- maximal force and failing part.**

Material \ Load Condition	PEEK	Ti
Pressure Load	24 kN, Bone not damaged	56 kN, Bone damaged (starting 42 kN)
Line Load	14 kN, Bone not damaged	75 kN, Bone damaged (starting 70 kN)

**Table 12. FEA results- maximal displacement**

Material \ Load Condition	PEEK	Ti
Pressure Load	1.5mm	0.7 mm
Line Load	2,3 mm	1,4 mm

Thus the *pressure load* analysis results showed that the Ti implant is much more resistant than the PEEK prosthesis. While a *PEEK implant breakthrough* was detected at a load magnitude of  $p = 8.5$  MPa, the *Ti prosthesis* assembly failed under a pressure of  $p = 20$  MPa.

Furthermore, the interaction behavior at the BII differed for the two materials. For the *PEEK implant* assembly, a *clear failure* of the *prosthesis without* significant effects on the bone or screws could be expected. In comparison, the load on a *Ti implant influenced the bone structure*. Several critical nodes near the skull drilling hole indicate that most probably small cracks will occur in this area. However, for the *Ti setup* a *screw failure* was calculated.

Based on experiences from crania-maxilla-facial surgeons a penetration of the implant up to a value of 2 mm into the meningitis could be considered as non-critical and Yonogadan N. measured failure deflections in their experiment with values between 8.9 and 15.4 mm. Both implant shifts are not critical and do not endanger the patient.

As for the *line load*, the Ti implant assembly withstood a much stronger impact than the PEEK setup. For *both materials the failing part is the implant*. However, a significant difference was given regarding the effect on the other setup parts. For the *PEEK assembly, neither the bone nor the screw* were not involved in the damage. In comparison, *the bone structure* of the *Ti setup* shows *damage at the BII near the drilling hole*. Although a breakthrough of the implant is assumed, the bone might be damaged significantly.

The comparison of the force deflection curve of the FEA and the experimental set up showed that the maximal forces were almost equal in all the cases. PEEK could withstand a force of 24.2 kN before fracturing. The titanium implant sustained a force of 45.8 kN before damage of the fixation screws and the polyamide skull model occurred. The sag of the titanium force-deflection curve before the structural failure can be explained by a non-centric loading of the implant with asymmetric force distribution. Minor cracks in the polyamid skull could have supported this curve

change. These data suggest the assumption that both materials used for the cranioplasty protect the brain as well as bone against mechanical trauma.

A great difference was seen in the deflection of the materials. This is due to the linear elastic material properties assumed in the FEA. Thus, in the FEA the maximal deflection was of 2.3 mm whereas in the experimental set up of 8.4 mm (PEEK). Whereas deflection of the PEEK implant could be observed with the high-speed camera, we did not observe this phenomenon in the titanium implants. The deflection measured in the titanium implants was a result of the skull model alone. This is explained by the higher elasticity of PEEK compared to Ti.

This study suffers from several possible limitations due to the assumed simplifications. However, due to the validated results, it is shown that this preliminary model could serve as a base for further studies.

## 5. Conclusion

A preliminary model was built to investigate the structural and failure behavior of a skull-implant set up. Both implants withstood forces which are higher than necessary to cause skull fractures (Yonagadan 1995). Keeping in mind all the simplifications that were assumed in this FEA, the maximal forces were validated by an experimental test rig. The calculated forces may seem very high. This could be due to the fact that the implemented Ti implants were much thicker than the ones used in the praxis. However, it is important to cite that such forces could occur during an impact (Broglio 2003). Due to PEEK's elasticity, which resembles bone more than that of titanium, there is the potential for better protection of the brain in case of traumatic stress. These findings - in addition to clinical advantages concerning patients comfort and follow-up in tumor patients - encourage further investigations.

Recent work aimed to implement *hyperelastic material models* for the PEEK implant as well as the PA base. Moreover the *load application area* was modeled according to the plate in the experimental set-up and a *dynamic simulation* was started. Moreover, effort is put in implementing a true anatomical geometry of the patient skull and customized implant by importing for example the parts as STL after scanning tomography.

## 6. References

1. Albrektsson T., Branemark P., Hansson H. and Lindstrom J." Osseointegrated Titanium Implants. Requirements for Ensuring a Long-Lasting, Direct Bone-to-Implant Anchorage in Man". Acta Orthop Scand 1981; 52, pp.155-70.
2. Barros R. et. al. "Effect of Biofunctionalized Implant Surface on Osseointegration – a Histomorphometric Study in Dogs". Brazilian Dental Journal 2009; 20, pp. 91-98.
3. Broglio S., Ju Y., Broglio M., Sell T. "The Efficacy of Soccer Headgear". J Athl Train 2003; 38, pp. 220-224.
4. Cabraja M., Klein M. and Lehmann T.N. "Long-Term Results Following Titanium Cranioplasty of Large Skull Defects". Neurosurg Focus 2009; 26:E10.
5. Debolé M., García, J. and Gomez M. "Modeling Bone Tissue Fracture and Healing: a Review". Eng Fract Mech. 2004; 7, pp. 1809-1840.

6. Eschbach L. "Nonresorbable polymers in bone surgery". *Injury* 2000; 31, Suppl 4, pp. 22-7.
7. Hughes T. "The Finite Element Method: Linear Static and Dynamic Finite Element Analysis". Dover Publications, 2000.
8. Katzer A., Marquardt H., Westendorf J., Wening J. and von Foerster G. "Polyetheretherketone-Cytotoxicity and Mutagenicity In Vitro". *Biomaterials* 2002; 23, pp.1749-59.
9. Lethaus B. et. al. "A Treatment Algorithm for Patients with Large Skull Bone Defects and First Results". *J Craniomaxillofac Surg* 2010, in press.
10. Li H, Ruan J., Xie Z., Wang H. and Liu W. "Investigation of the Critical Geometric Characteristics of Living Human Skulls Utilising Medical Image Analysis Techniques". *Int. J. of Vehicle Safety* 2007; 2 (4) pp. 345-367
11. Motherway J., Verschueren P., Van der Perre G., Vander Sloten J. and Gilchrist M. "The Mechanical Properties of Cranial Bone: The Effect of Loading Rate and Cranial Sampling Position". *Journal of Biomechanics* 2009; 42, pp. 2129-2135.
12. Simulia: Abaqus User's Manuel. 2007, V. 6.7
13. Simulia: Abaqus User's Manuel. 2008, V. 6.8
14. Spetzger U., Vougioukas V. and Schipper J. "Materials and Techniques for Osseous Skull Reconstruction". *Minimally Invasive Therapy* 2010; 19, pp. 110-121.
15. Winder J. "Computer Assisted Cranioplasty". *Virtual Prototyping Biomanufacturing in Medical Applications*. Berlin: Springer Verlag 2007; pp.1-20.
16. Yoganandan N. et. al. "Biomechanics of skull fracture". *J Neurotrauma* 1995; 12, pp.659-68.

## 7. Acknowledgment

We would like to thank IDEE Maastricht, especially Paul Laeven and Maikel Beerens for their support in the production of the CAD-models and the testing implants. We also like to thank the Institute of Geotechnical Engineering (RWTH Aachen) for the performance of the experimental validation pressure-tests.